Proceedings of the Fifth International Symposium
on
Advanced Nuclear Energy Research
—NEUTRONS AS MICROSCOPIC PROBES

I—22

APPLICATIONS OF POLARIZED NEUTRONS

F. MEZEI

BENSC, Hahn-Meitner-Institut, Pf. 390128, 14091 Berlin

ABSTRACT

The additional spin degree of freedom of the neutron can be made use of in neutron scattering work in two fundamental ways: (a) directly for the identification of magnetic scattering effects and (b) indirectly as a spectroscopic tool for modulating and analysing beams. Although strong magnetic scattering contributions can often be studied by unpolarized neutrons, a fully unambiguous separation of nuclear and magnetic phenomena can only be achieved by the additional information provided by polarized neutrons, especially if one of the two kinds of contributions is weak compared to the other. In the most general case a sample with both magnetic and nuclear features can be characterized by as many as 16 independent dynamic correlation functions instead of the single well known S(q,ω) for non-magnetic nuclear scattering only. Polarization analysis in principle allows one to determine all these 16 functions. The indirect applications of polarized neutrons are also steadily gaining importance. The most widely used method of this kind, the application of Larmor precessions for high resolution energy analysis in Neutron Spin Echo spectroscopy opened up a whole new domain in inelastic neutron scattering which was not accessible to any other spectroscopic method with or without neutrons before.

INTRODUCTION

The utilization of spin polarized neutron beams in neutron scattering work was started in 1951 by C.G. Shull's diffraction study of magnetite [1], although the theoretical foundations had been laid much earlier, shortly after the discovery of the neutron [2]. Since then polarized neutrons have become a traditional accessory of neutron diffraction investigation of primarily ferromagnetic and ferrimagnetic samples, which can be fully magnetized. Inelastic magnetic processes, such as magnons, could also be singled out by polarized neutrons in the same class of samples, although this has really been done much less often. I shall not include these classical applications in the present survey, but rather concentrate on a few selected, more recently introduced approaches, which appear to make part of emerging trends of increasing importance in the future. This rather arbitrarily chosen list of recent highlights includes

1.) general vectorial (or 3 dimensional) polarization analysis studies of magnetic structures
2.) determination of generalized and local magnetic susceptibilities in paramagnets

3.) generalized Neutron Spin Echo (NSE) spectroscopy for the investigation of phonon lifetimes.

To start with, a short reminder will be presented in order to review the current situation with polarizer and analyser systems from the point of view of availability and performance.

POLARIZERS AND ANALYSERS: STATE OF THE ART

The extra information obtainable by the observation of the dependence of a neutron scattering cross section on the neutron beam polarization (called "scattering of polarized neutrons") or by determination of the scattered beam polarization as a function of the incoming beam polarization (called "polarization analysis") is usually rather dearly paid for by a loss in beam intensity. This particularly handicaps polarization analysis, where both polarizer and analyser are needed. The undue intensity loss is primarily related to the limited beam divergence accepted by polarizers (e.g. insufficient mosaic for crystals or small critical angle for mirrors). Supermirrors with a critical angle of about 0.2 deg per Å wavelength provide a satisfactory solution for $\lambda \gtrsim 3Å$, and this wavelength limit might be improved in the future, if higher critical angle mirrors become available in sufficient quantities. In particular, supermirror polarizers can handle the full beam divergence contained in a standard Ni coated guide with losses smaller than about 30 % (beyond the 1/2 spin population factor). This is examplified by the beam splitter polarizer system, which is presently set up at one of the neutron guides at BENSC in Berlin [3]. Here the neutrons are selected according to their spin state into two beams serving two instruments. Both beams offer a broad wavelength band with uniformly high polarization and transmission coefficients (Fig. 1).

The situation is less satisfactory with analysers, although Soller type supermirror systems can in principle be put together into analysers with large solid angle acceptance. The problem is the quantity of supermirrors required: in order to cover 1 m^2 of detector area an analyser system for $\lambda \gtrsim 3Å$ will consist of some 60 – 200 m^2 of supermirrors depending on the lay-out, i.e. some 3 to 10 years production of a $ 1 Mio vacuum deposition machine. The largest solid angle analyser set in existence today is the one on D7 spectrometer [4] at ILL covering about 0.1 m^2 total detector surface (32 detectors) using some 25 m^2 of supermirrors, the deposition of which took over 4 full years for W. Graf working with O. Schärpf. The largest area single analyser element is the one used on the NSE spectrometer IN 11 with an area of about 9×9 cm^2 containing 0.6 m^2 of supermirrors [5]. On each of these instruments the counting rate in each detector in a polarization analysis experiment is at least 2 times superior at a wavelength of 5Å compared to the best existing thermal triple axis spectrometers at the peak of the polarized flux. This means for D7 2 orders of magnitude higher data rates, however without energy analysis and with the additional limitation that due to the use of cold neutrons only relatively slow magnetic fluctuations can be studied efficiently (up to few *meV*).

For shorter wavelengths thermal neutrons the hope of producing graphite quality Heusler crystal polarizes has still not been fulfilled beyond a few lucky strikes of insufficient number. The relatively large d spacing, *3.35 Å* also is a drawback for the resolution both in diffraction and in inelastic spectroscopy. A promising real breakthrough is seen now in developing non-monochromatizing polarized ^3He gas filters, which will work in a broad wavelength range including $\lambda \leq 1Å$. This kind of filters are being developed for

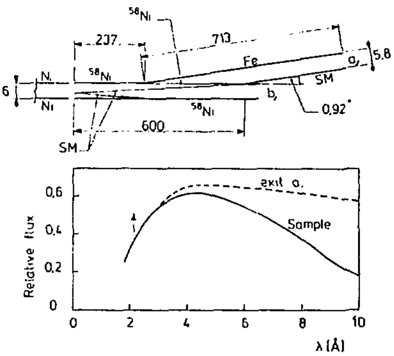

Fig. 1. Large wavelength band polarizer–beam splitter neutron guide section under construction at BENSC (dimensions in cm) [3].

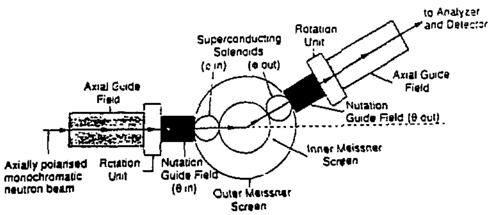

Fig. 2. Schematic layout of the 3 dimensional vector polarization analysis CRYOPAD at ILL [10].

nuclear physics experiments with considerable effort and although there are encouraging results, it is not at all clear by now if the cell size and stability required for sensible neutron experiments will become attainable any soon at affordable costs.

FUNDAMENTALS

Conventional polarization analysis as introduced decades ago [6] is only concerned with one component of the neutron spin polarization vector, say P_z, where z is parallel to the field direction on the sample. Thus the polarization can be defined in terms of the occupation numbers $n_\uparrow$ and $n_\downarrow$

$$P_z = n_\uparrow - n_\downarrow \tag{1}$$

where "up" and "down" refer to the z direction and $n_\uparrow + n_\downarrow = 1$. In this description the scattering process can be fully accounted for by 4 partial cross sections t_{ij}, which are in fact the transition probabilities between neutron spin states i to j ($i,j=\uparrow,\downarrow$), and the scattered beam polarization $P'_z = n'_\uparrow - n'_\downarrow$ is given by the matrix equation

$$\begin{pmatrix} n'_\uparrow \\ n'_\downarrow \end{pmatrix} = \begin{pmatrix} t_{\uparrow\uparrow} & t_{\downarrow\uparrow} \\ t_{\uparrow\downarrow} & t_{\downarrow\downarrow} \end{pmatrix} \begin{pmatrix} n_\uparrow \\ n_\downarrow \end{pmatrix} \tag{2}$$

Thus, this scalar approach can provide 4 independent parameters about the sample, which are actually functions of the momentum and energy transfer variables $(\vec{q},\omega)$. This is a tremendously reduced picture, since the neutron spin, and therefore the neutron polarization in general is a 3 dimensional vector, and the interaction between neutron and sample is a tensor. In Ref. [7] it has been recapituled in detail that the $S = \frac{1}{2}$ character of the neutron spin leads to a maximum of 16 cross sections, which are independent of each other in the spin variable and can theoretically all be determined by the vector polarization analysis methods. It is interesting to note that a generally overlooked piece of experimental work at St. Petersburg (Leningrad then) demonstrated the feasibility of vector polarization analysis [8] before the scalar variant was described at Oak Ridge. The most widely used example of vector polarization work yet is NSE spectroscopy [9].

Just to summarize (for details see Ref. [7]), the wavenumber dependent Hamiltonian potential for the neutron scattering process is:

$$V = -\vec{\mu}B(\vec{q}) + \sum_i e^{iqr_i}(b_i + a_i\vec{I}_i\vec{\sigma}) \tag{3}$$

where $\vec{\mu} - 1.913\mu_N\vec{\sigma}$ is the neutron spin, and the sum goes over the nuclei in the sample. Following Maxwell's equations the Fourier transform of the magnetic field $\vec{B}$ can be expressed by the magnetization $\vec{M}$:

$$\vec{B}(\vec{q}) = \vec{M}(\vec{q}) - [\vec{q}\vec{M}(\vec{q})]/q^2 \tag{4}$$

Eq.(3) leads to transition probabilities (cross sections) of the most general form

$$|< \lambda', \chi' \mid b(\vec{q}) + \vec{a}(\vec{q})\vec{\sigma} \mid \lambda, \chi >|^2 \tag{5}$$

where λ, χ are the initial states of the sample and the neutron spin, respectively, and λ', χ' are the final states. For any transition $\lambda \rightarrow \lambda'$ this scattering matrix element depends on 4 complex numbers: $< \lambda' \mid b(\vec{q}) \mid \lambda >$ and $< \lambda' \mid \vec{a}(\vec{q}) \mid \lambda >$, i.e. 7 parameters with one phase being fixed arbitrarily. In an ideal sample, Bragg scattering processes are good conceptional examples for single state transitions: λ and λ' can be taken equal to an effective "ground" state λ_0. Thus, in magnetic crystallography one has to be able to determine 7 independent parameters by polarization analysis. Thus the scalar approach is insufficient. This does not imply that 7 spin parameters per Bragg reflection are sufficient to determine the structure, but that they contain all information visible to the $S = \frac{1}{2}$ neutron.

Realistic samples are most often magnetically not monodomain and the manifold of thermally excited states are also to be taken into account in the determination of the Debye-Waller factors and diffuse scattering processes. Consequently, we cannot only consider a single transition matrix element $\lambda \rightarrow \lambda'$ in eq.(5) but have to average over the initial states λ and the sum over the final states λ'. This process leads to 16 independent correlation functions: $< b^*b >$, $< a^*_\alpha a_\alpha >$, $Re < b^*a_\alpha >$, $Im < b^*a_\alpha >$, $Re < a^*_\alpha a_\beta >$, $Im < a^*_\alpha a_\beta >$, where $\alpha \neq \beta$. Let us recall that all of these correlation functions are functions of $\vec{q}$ and ω.

Finally it remains to recall that these 16 independent correlation functions can really be experimentally determined. The polarization dependence of the scattering cross section can most generally be written in the form of

$$\frac{d^2\sigma}{d\Omega d} \propto A(\vec{q},\omega) + \vec{B}(\vec{q},\omega)\vec{P} \tag{6}$$

where A and $\vec{B}$ are a real scalar and a real vector, respectively. In the same manner the scattered beam polarization is obtained as

$$\vec{P}_f\frac{d^2\sigma}{d\Omega d\omega} \propto \vec{C}(\vec{q},\omega) + \mathcal{T}(\vec{q},\omega)\vec{P} \tag{7}$$

where $\vec{C}$ is a real vector and $\mathcal{T}$ a real ternsor. These linear equations would be a first approximation for classical ($S\rightarrow \infty$) spins, but for $S = \frac{1}{2}$ higher order terms do not exist.

A, $\vec{B}, \vec{C}$ and $\mathcal{T}$ are the measurable quantities and they represent exactly 16 independent components. It can be shown that the equations expressing the above 16 correlation functions in terms of these 16 measurable parameters can be uniquely solved [7]. Thus vector polarization analysis makes accessible all information on the scattering potential the neutron can see at all.

VECTOR POLARIZATION ANALYSIS

After the pioneering work of the St. Petersburg group and some further partial results and proposals a new set-up has been developed by F. Tasset and co-workers at ILL [10], which allows to perform the vectorial polarization measurements as defined by eqs.(6) and (7) for the first time with sufficient precession at any scattering angle. The apparatus dubbed CRYOPAD is an extremely elaborate set of guidefields, precession and flipper coils and superconducting shields (Fig. 2). A first set of beautiful experiments could be completed before the shut down of ILL, e.g. correction of earlier proposed magnetic crystal structures by revealing the complex non-collinear nature of the magnetic order [11].

GENERALIZED AND LOCAL SUSCEPTIBILITIES IN PARAMAGNETS

In order to understand the magnetic susceptibility of paramagnets with strong interactions (e.g. strongly correlated electron systems) the temperature dependence of the susceptibility provides too little clue, actually in form of deviations from the Curie law $\chi(T) \propto \frac{1}{T}$. Such deviations are either due to a temperature dependence of the localized magnetic moments (e.g. Kondo effect) or to correlations between neighbouring magnetic moments. These correlations are expressed by the generalized susceptibilities $\chi^{\alpha\beta}(\vec{q})$, which describe the β component of the response induced by the α component of a staggered field. For systems with reasonable symmetry properties only $\alpha=\beta$ contributions are not negligible, and the relation between susceptibility and neutron scattering cross section due to the α component of the paramagnetically fluctuating moments reads [12]

$$\chi^{\alpha}(\vec{q}) \; \alpha \; \frac{1}{kT}\left(\frac{d\sigma}{d\Omega}\right)^{\alpha}_{PM} \tag{8}$$

This equation holds in the quasielastic approximation only, i.e. if the neutron energy change is small compared to both the initial neutron energy and to kT. This is also a practical condition for directly determining the cross section $d\sigma(\vec{q})/d\Omega$ by collecting neutrons without energy analysis like in ordinary two axis diffraction, since the energy integration of $d^2\sigma(q,\omega)/d\Omega d\omega$ usually is a hopeless task with the low intensities involved. One of the main reasons why higher energy polarized neutrons would be so valuable, is just to achieve safer energy integration of the scattering response.

The problem of determining $\chi^{\alpha}(\vec{q})$ via eq.(8) is the high background of nuclear (incoherent, multiple-Bragg, phonon and multiphonon) scattering. Polarization analysis offers a straightforward solution in macroscopically isotropic samples: $\chi = \chi^{\alpha}, \alpha = x, y, z$. The isotropic magnetic behaviour will result in a characteristically anisotropic polarization behaviour with respect to $\vec{q}$ due to the second term in eq.(4), while the other

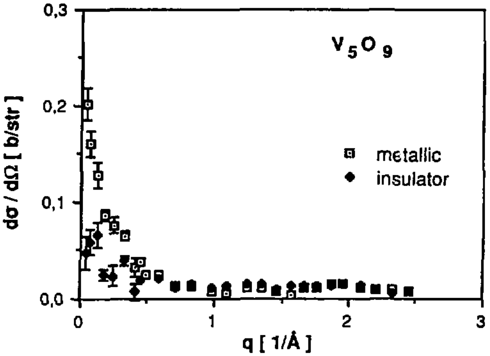

Fig. 3. Signature of ferromagnetic shortrange order in the generalized susceptibility of V_5O_9 [13].

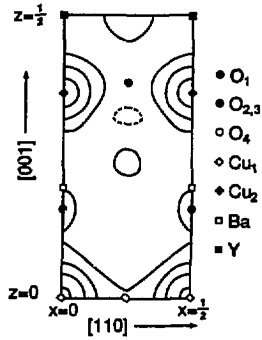

Fig. 4. Distribution of local magnetization induced in a $Y - Ba - Cu - O$ sample by a *4.6 T* field [16].

contribution to the $\vec{a}(\vec{q})$ vectorial term in (5), the nuclear spin interaction $\vec{I}_i\vec{\sigma}$ in eq.(3) remains isotropic. The result is the famous Halpern-Johnson equation $\vec{P}' = -\vec{q}(\vec{P}\vec{q})/q^2$ for the paramagnetic response, and $\vec{P}' = -\vec{P}/3$ for the nuclear spin response. The scalar term in (5) leads to $\vec{P}' = \vec{P}$. To sort out a sum of these three types of behaviour it is sufficient to determine the 3 diagonal elements of the tensor T of eq.(7) in a coordinate system adequately chosen in view of the possible directions of $\vec{q}$ [9].

A recent example [13] is shown in Fig. 3. The generalized susceptibility $\chi(q)$ has been determined in the metallic *(T>170 K)* and insulating phases of a V_5O_9 powder sample, using D7 and IN11 spectrometers at ILL. The macroscopic susceptibility $\chi(q{=}0)$ shows a jump at the metal–insulator transition from an expected $2.1\mu_B/per\ V\ atom$ Curie behaviour in the metallic phase to some 3 times smaller value. Up to now this has been interpreted as an onset of antiferromagnetic nearest neighbour correlations in a Mott type insulator phase. The neutron results reveal that quite to the contrary, the atomic moments in the metallic phase are rather small ($\sim 0.6\mu_B$) and the higher susceptibility is due to ferromagnetic correlations. Thus we rather have to do with an itinerant, strongly correlated electron metal and not with quasi-free atomic moments.

In strongly temperature dependent phenomena, e.g. critical scattering above a phase transition, the requirement of isotropic sample behaviour can be dropped under the assumption that the nuclear background is temperature independent so that the identification of the nuclear and magnetic contributions can be performed by the above approach at a high enough temperature, where the sample can be considered isotropic. Then, above a now well known background, the temperature dependent anisotropy can be observed within the plane perpendicular to $\vec{q}$, the magnetization component parallel to $\vec{q}$ being cancelled in eq.(4). In a single crystal near to a Bragg peak full anisotropy studies are also possible since here χ^α will depend on the reduced variable $\vec{q}_r = \vec{q} - \vec{\tau}_{hkl}$, (which can e.g. be perpendicular to $\vec{q}$), while the total momentum transfer $\vec{q}$ applies to eq.(4). This way it was possible to determine the predicted dipolar anisotropy of the critical fluctuations at the Curie point of isotropic ferromagnets [14], i.e. to show that only $\chi^{\perp}(\vec{q})$ diverges critically, while $\chi^{\parallel}(\vec{q})$ tends to a constant as $q \rightarrow 0$ and $T \rightarrow T_c$. Here $\perp$ and $\parallel$ stand for parallel and perpendicular to $\vec{q}$. (This experiment also only implies the determination of diagonal elements of the tensor $\mathcal{T}$.) More recently, the more difficult task of determining the dipolar anisotropy of the inelastic critical scattering $d^2\sigma/d\Omega d\omega$ has also been accomplished by the same polarization analysis trick [15].

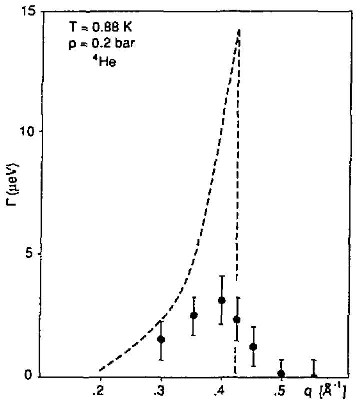

Fig. 5. Phonon linewidth due to spontaneous phonon decay in superfluid ^4He at $T \rightarrow 0$ [18].

The determination of the local susceptibilities, on the other hand, is a generalization of polarized neutron crystallography, making use of improved efficiency of the instruments. A high magnetic field is applied to paramagnetic samples introducing a polarization corresponding to the $\chi(q=0)$ susceptibility. The distribution of this induced magnetic density is then determined in the form of magnetization maps by single crystal diffraction methods. The results allow to identify the contribution of individual atomic sites to the total magnetization with the impressive sensitivity of $< 0.001\ \mu_B/atom$. Fig. 4 shows an example obtained in Y-Ba-Cu-O [16]. The higher polarizability of the Cu atoms on the chain sites compared to the antiferromagnetically coupled Cu in the planes and the contribution of O sites are the marked features put to evidence.

GENERALIZED NEUTRON SPIN ECHO SPECTROSCOPY

In common applications of Neutron Spin Echo (NSE) spectroscopy quasielastic scattering processes are investigated with a high resolution of some *0.01* μeV (sensitivity even higher) corresponding to characteristic times of up to 10^{-7} *sec*. This has opened up a new field of applications of neutron scattering spectroscopy in the study of slow processes. An similarly important extension of the capabilities of neutron methods can be expected from the generalization of NSE for the studies of elementary excitations first proposed in 1977 and demonstrated in 1979 [9, 17]. The method, however, has only been applied in a very small number of real experiments on superfluid ^4He, due to technical difficulties and to the small capacity available for tackling such difficulties in the physcis community busily producing publications on a faster pace than technical development work is likely to permit. The latest example of these few results is shown in Fig. 5 [18]. The lifetime of phonons in superfluid ^4He at $T<1\ K$ is dominated by the anharmonic decay of one phonon into two others. At low pressures these processes are kinematically only allowed for $q \leq 0.43\ \AA^{-1}$, due to the particular shape of the dispersion relation. The energy resolution in this example is better than 10^{-3}, i.e. nearly two orders of magnitude better than the some 50 μeV available by conventional spectroscopy. Because such a resolution improvement would imply an intensity loss by a factor of some 10^4 or more using conventional methods, the focussing feature of the NSE approach offers the only possible way to avoid this kind of intensity penalty.

The technical difficulty of generalizing NSE for the study of elementary excitations (beyond obtaining a reasonable flux in polarization analysis) resides in the necessity to tune the shape of the precession fields too [9, 17]. This technical problem can be solved much easier by the recently developed Zero Field NSE trick [19] (which is based on the use of r.f. flippers instead of the d.c. ones in ordinary NSE) and it is to be expected that the results of the work in progress in collaboration of TU Munich and BENSC on the implementation of ZF-NSE on a triple axis instrument will make this kind of studies more generally accessible and feasible.

REFERENCES

[1] C.G. Shull, E.O. Wollan, and W.A. Strauser, Phys. Rev. **81** (1951) 483.
[2] F. Bloch, Phys. Rev. **50** (1936) 259, and **51** (1937) 994.
[3] F. Mezei, in: Thin Film Optical Devices, C. Majkrzak (ed.), SPIE proc. vol. 983 (Bellingham, 1989), p. 10.
[4] O. Schärpf: Physica B **156-157** (1989) 639.
[5] F. Mezei, in: Supplement to Atomenergie-Kerntechnik **44** (Karl Thiemig, München 1984) p. 735.
[6] R.M. Moon, T. Riste, and W.C. Koehler, Phys. Rev. **181** (1969) 920.
[7] F. Mezei, Physica **137B** (1986) 295.
[8] G.M. Drabkin, E.I. Zabidorov, Ya. A. Kasman and A.I. Okorokov, JETF Pisma **2** (1965) 541, and Zh. Eksp. Teor. Fiz. **56** (1969) 478.
[9] F. Mezei, Z. Phys. **255** (1975) 146, and in: Neutron Spin Echo, F. Mezei (ed.), (Springer Verlag, Heidelberg 1980) p. 3.
[10] F. Tasset, Physica B **156-157** (1989) 627.
[11] P.J. Brown, V. Nunez, F. Tasset, J.B. Forsyth, and P. Radhakrishna, J. Phys. Condensed Matter **2** (1990) 9409.
[12] See W. Marshall and S.W. Lovesey, Theory of Thermal Neutron Scattering (Clarendon, Oxford, 1971).
[13] F. Mezei, P. Canfield, and O. Schärpf, Physica B **180-181** (1992) 361.
[14] J. Kötzler, F. Mezei, D. Görlitz, B. Farago, Europhys. Lett. **1** (1986) 675.
[15] P. Böni, D. Görlitz, J. Kötzler, and J.L. Martinez, Phys. Rev. B **43** (1991) 8755.
[16] J.X. Boucherle, J.Y. Henry, M.J. Jürgens, J. Rosset-Mignod, J. Schweizer, F. Tasset, Physica C **162-164** (1989) 1285.
[17] F. Mezei, Phys. Rev. Lett. **44** (1980) 1601.
[18] F. Mezei, C. Lartigue, and B. Farago, in: Excitations in Quantum Fluids, A.F.G. Wyatt and H.J. Lauter (eds.), (Plenum, New York, 1991) p. 119.
[19] R. Golub and R. Gähler, Phys. Lett. A **123** (1987) 43 and J. Phys. **49** (1988) 1195.